INTERNATIONAL JOURNAL OF HYDROGEN ENERGY 36 (2011) 3067–3075

Available at www.sciencedirect.com

ScienceDirect

journal homepage: www.elsevier.com/locate/he

Diagnosis of polymer electrolyte fuel cells failure modes (flooding & drying out) by neural networks modeling

N. Yousfi Steiner [a,*], D. Hissel [b], Ph. Moçotéguy [a], D. Candusso [c]

[a] EIFER, European Institute for Energy Research, Emmy-Noether Str. 11, Karlsruhe, Germany
[b] FEMTO-ST/ENISYS/FCLAB, UMR CNRS 6174, University of Franche-Comté, rue Mieg, 90010 Belfort Cedex, France
[c] INRETS/FCLAB, The French National Institute for Transport and Safety Research, rue Mieg, 90010 Belfort Cedex, France

ARTICLE INFO

Article history:
Received 19 July 2010
Received in revised form
23 September 2010
Accepted 24 October 2010
Available online 8 January 2011

Keywords:
PEM Fuel cell
Diagnosis
Flooding
Drying out
Degradation
Elman neural network

ABSTRACT

Fault diagnosis and durability of Polymer Electrolyte Fuel Cells (PEFCs) have been identified among the critical issues that need to be overcome for a commercial viability of these power sources.

Fuel cells fault diagnosis requires the knowledge of a number of fundamental parameters such as applied current, air inlet flow rate Q, stack temperature and dew point temperature that usually need a special monitoring system and a specifically adapted fuel cell geometry. This might be difficult and even impossible in many fuel cell stacks. Such a constraint could only be possible in a laboratory setup and is not adapted to real application. Moreover, for the transportation application, which aims at minimizing the embedded instrumentation, simple diagnosis methods involving non-intrusive and easy-to-monitor parameters are highly desired.

This paper presents a diagnosis procedure of water management issues in fuel cell, namely flooding and drying out, based on a limited number of parameters that are, besides, easy-to-monitor.

This procedure uses a black-box model based on neural networks that simulates, in case of healthy operation, the evolution of pressure drop at the cathode as well as fuel cell voltage. Two residuals are generated from the comparison between the actual operation of the fuel cell and the parameters calculated by a neural network in case of normal operation.

The two residuals analysis permits the detection (by the means of comparison with a predetermined threshold) and the classification of fuel cell's states-of-health between flooding, drying out or normal operation.

1. Introduction

Polymer Electrolyte Fuel cells (PEFCs) convert directly the chemical energy of hydrogen into electrical energy with high efficiency, without CO_2 emission (when the fuel is cleanly produced) releasing only heat and water. However, the PEFC is still not commercially viable. Fault diagnosis and durability of PEFC are identified as part of the critical issues that need to be overcome for a commercial viability of these power sources.

This is why, in the last few years, the interest in understanding the degradation mechanisms and the diagnosis methodologies is growing [1–3].

PEFC fault diagnosis needs traditionally the knowledge of a number of inner parameters concerning the operation, the

* Corresponding author. Tel.: +49 72161051338; fax: +49 72161051332.
E-mail addresses: nadia.steiner@eifer.org (N. Yousfi Steiner), daniel.hissel@univ-fcomte.fr (D. Hissel), philippe.mocoteguy@eifer.org (Ph. Moçotéguy), denis.candusso@inrets.fr (D. Candusso).
0360-3199/$ – see front matter © 2010 Professor T. Nejat Veziroglu. Published by Elsevier Ltd. All rights reserved.
doi:10.1016/j.ijhydene.2010.10.077

Nomenclature

I	current
P_{H_2O}	partial pressure of water
$P_{H_2O,sat}$	saturation pressure
Q	air flow rate
T, T_{stack}	stack temperatute
T_{dwpt}	inlet gas dew temperature
$\hat{U}$, U_{calc}	voltage calculated by the neural network
U_{exp}	measured value of the voltage
$\Delta\hat{P}$, ΔP_{calc}	pressure drop calculated by the neural network
ΔP_{exp}	measured value of the pressure drop
$\sigma(\bullet)$	standard deviation
$\varepsilon_{\Delta P}$, ε_U	residual value calculated respectively on the pressure drop and voltage
$s_{\Delta P}$, s_U	threshold value calculated respectively on the pressure drop and voltage
λ	water content of the membrane
Φ_{in}	relative humidity at inlet

geometry as well as materials. In fact, an efficient control and supervision of a fuel cell system depends on the proper understanding and behavioral representation of the processes occurring both in the stack and between the stack and its ancillaries. In this regard, modeling and experimentation are efficient tools. A good knowledge of the influent parameters in the cell operation is therefore necessary, but the lack of adequate tools for monitoring fuel cell inner parameters is a hurdle to the cell active control. Moreover, for transportation application, which aims at minimizing the embedded instrumentation, simple diagnosis methods involving non-intrusive and easy-to-monitor parameters are highly desired.

There are many different approaches for fault diagnosis of PEFC stacks. These approaches could be either based on a model (behavioral model, mathematical models, etc.) [4] or based on experimental data and knowledge. Impedance measurements, for example are very used tools to water management issues diagnosis. Merida et al. [5] for instance, used this technique in order to investigate flooding and drying out issues in a four-cell stack. The two faults could be separated by operating the impedance measurement in a separate frequency range. On an other work, Roy et Orazem [6] used impedance spectroscopy measurement and the stochastic character of the flooding for a robust diagnosis. Their work shows the potential of impedance error analysis methodology for drying out and flooding detection.

The "behavioral models", which resort to a "black-box" representation of the system admit some input variables and evaluate the output values. These models are fast to implement and overcome the strong limitation of physical ones that use the mathematical equations describing the actual physical phenomena occurring in each fuel cell's components and which need an accurate identification of the PEFC inner parameters (relating to operation, geometry and materials).

Among those "black-box" models, many are based on Neural Networks (NNs), which have many advantages. They can indeed learn and approximate any continuous nonlinear function and does not need the knowledge of the physical process behind it. They however need good quality data, which means data describing the whole process to be modeled. When they are properly trained, the NNs have strong capacity to model complex nonlinear mapping with accuracy.

In fuel cells, the complexity to describe precisely the entire physical phenomenon makes the NNs very attractive tools. Some researchers used it in fuel cell systems for different purposes [7–9]: Jemeï et al. [7] developed a dynamic NN in order to control a PEFC system process. Kumbur et al. [8] used NN-based model in order to predict the capillarity mechanisms in the diffusion media, mainly reflected by the capillarity pressure, from correlated parameters based on the non-wetting phase saturation, namely the compression pressure and the PTFE content in the gas diffusion layers. More recently, Lobato et al. [9] presented a study of the performance of a polybenzimidazole-based PEFC operating at 100–175 °C in function of operating conditions using three types of neural networks.

The authors present in this paper a procedure related to the diagnosis of water management issues: drying out and flooding. This procedure is based on recurrent neural networks. The inputs of the NN are critical variables for the performance and the outputs are relevant variables to detect and identify the PEFC current state-of-health.

The model-based NN achieves a nonlinear relationship between voltage and pressure drop on the one hand and current, flow rate, stack and dew point temperature in case of normal operation on the other hand (Normal operation is defined as non-flooded and non-dried fuel cell [6]). The model calculates the stack voltage and pressure drop in case of healthy operation. The procedure compares the model outputs with those measured from the system, in order to generate residuals. The analysis of obtained residual permits the detection of a default followed by an identification step.

This paper is organized as follow: paragraph 2 discusses the PEFCs faults linked to a bad water management. The tested stack, the bench as well as the different experiment performed in the frame of this work are described in Section 3. The diagnosis procedure is then presented in paragraphs 5 and 6. Finally, some results are presented in Section 6 and we conclude this work in Section 7.

2. Water management issues in fuel cells

Proton Exchange Membrane Fuel Cell is composed of two electrodes (anode and cathode) in contact with a membrane separating gas compartments fed by reactive gases (humidified hydrogen and oxygen or air). During its operation, the fuel cell delivers current and produces water inside the Membrane Electrode Assembly (MEA). Details about the operation of PEFC could be found in Ref. [10].

In a fuel cell, failure can be caused by long time operation (natural ageing) or by operation incidents, such as MEA contamination or reactant starvation [11,12]. A common consequence to all "fault" incidents is a voltage drop. Voltage is therefore a first indicator of degraded state.

The operation incidents linked with water management (cells flooding and membrane drying out) are of particular interest because they frequently occur during fuel cell operation and cause rapid power decay. They can even lead to irreversible chemical and mechanical degradation (of the membrane in case of drying out and of the catalyst in case of flooding) [1,3]. Flooding events, for instance, occur when stack temperature is below reactant gas' dew point temperature. The dew point temperature is the one below which a part of water contained in the reactant gas condensate into liquid, due to gas saturation (its relative humidity equals 100%). At constant pressure, relative humidity is directly linked with operating temperature: the closer dew point and operating temperatures are, the higher the relative humidity is. In this work, the relative humidity is controlled by both gases dew point and stack operating temperatures.

A characterization of flooding and drying out is done as a first step to the fault diagnosis (Fig. 1). The operating conditions and parameters that have a large impact on these phenomena, as well as the contribution of each factor, are discussed in a previous paper [2]. Fig. 1 represents fault trees that provide a better insight into the PEM flooding and drying out issues.

Widely used in operating safety and reliability science, the fault tree analysis (FTA) enables to clear out the different contributions. It is a "top-down" approach starting with a top event (undesirable event failure, malfunction…) and determining all the causes that can lead to it. The analysis proceeds

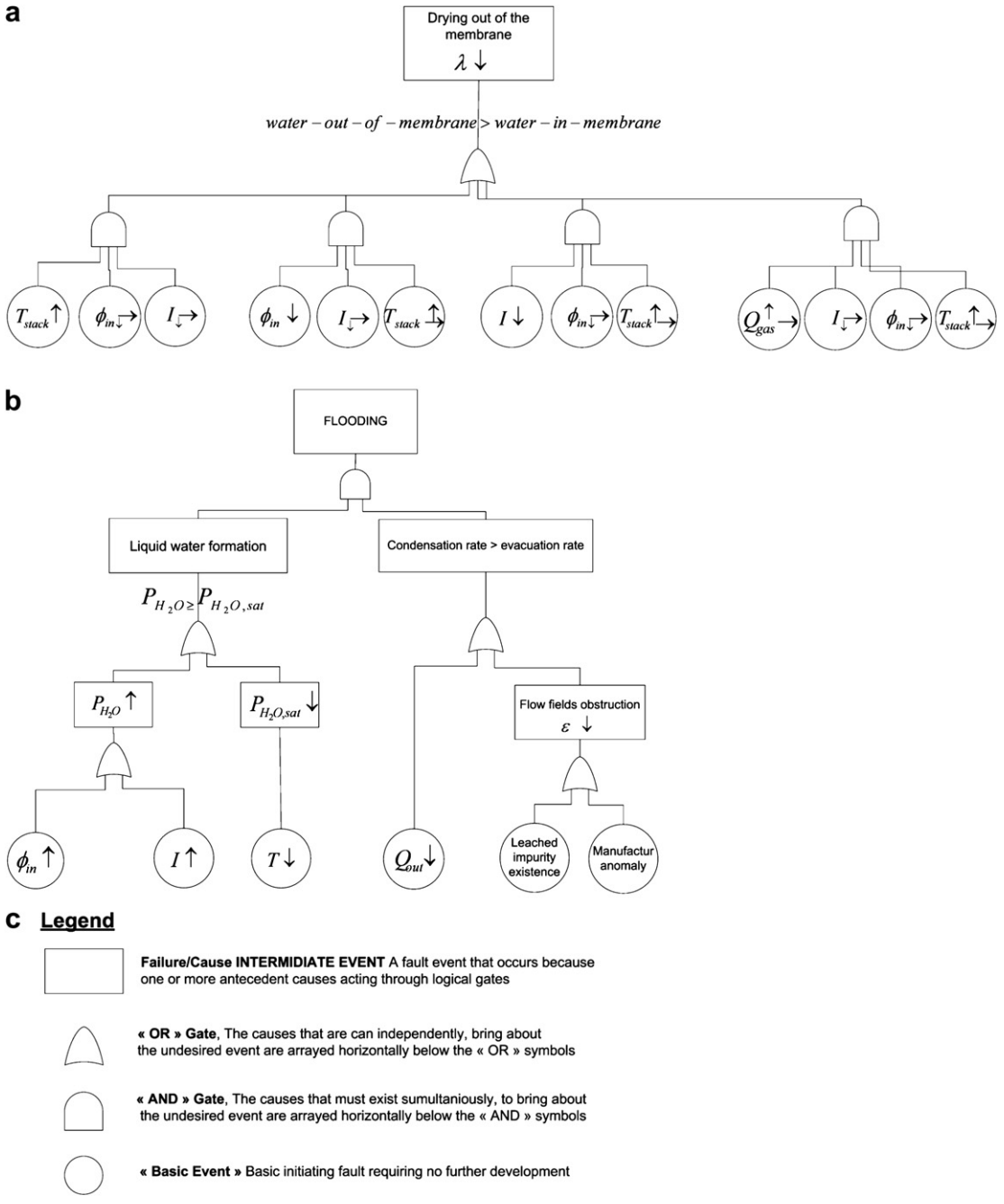

Fig. 1 – Fault trees linked to water management issues in PEFCs [2].

by determining how this top event can be caused by individual or combined lower level failures or events [13].

In the present study, four operating parameters influencing water management in PEFC are considered (those that are in the final "leaves" of the tree): air inlet flow rate Q, fuel cell temperature T, air dew point temperature (reflecting the relative humidity at the cathode, ϕ) and current I. Any change in one of these parameters impacts water management, leading to fault occurrence, mitigation or intensity modification. Therefore, these parameters are chosen as inputs for our model.

Concerning outlet parameters, besides voltage evolution, which will play the role of "degradation detector", the pressure drop between the channels inlet and outlet is the parameter that will discriminate between a flooding and a drying out. In fact, several studies have pointed out this parameter's relevance to reflect the liquid water accumulation and removal [14,15]. It is the result of the mechanical nonconservative interactions on gas particles. More details about the relevance of this parameter could be found in references [14–16].

3. Experimental setup presentation

3.1. Description of the test bench

A detailed description of the 1 kW PEFC test bench used for the endurance test can be found in Ref. [17]. Many physical parameters impacting stack performances can be controlled and measured in order to master the FC operating conditions as accurately as possible. Stack temperature, gas flow rates, fluid hygrometry rates, air dew point temperature and load current can be imposed. Inlet and outlet flow rates, pressures, temperatures and single cell voltages can be monitored.

At cathode side, the humidification system permits to set the inlet gases dew point temperatures. The gas is introduced in a water tank and saturate with water vapour at a fixed dew point. The gas is then heated to the set temperature prior entering into the fuel cell.

3.2. Fuel cell stack specifications

The fuel cell used in this study has experienced a succession of flooding and drying out. The PEM fuel cell has 20 cells with 100 cm^2 surface area. The stack has been assembled with commercial MEAs (Gore MESGA Primea Series 5510) and graphite distribution plates and the operating temperature is within the range 20–65 °C.

Table 1 summarizes the main technical characteristics of the fuel cell used in this work.

3.3. Flooding and drying out experiments description

The normal, flooding and drying out experiments have been simulated under different operating conditions: gas dew point temperature is varied in the range of 25–50 °C, current in the range of 0–35 A and the air flow rate in the range of 30–55 Nl min^{-1}.

The flooding states were experimentally simulated by increasing inlet gas dew point temperature so that water condensation is favored. The correlation between dew point temperature increase and fuel cell voltage decrease indicates the presence of flooding [14,15], since the power decay is quite fast and no other parameter is changed. Unlike flooding, the drying out is simulated by decreasing inlet gas dew point temperature so that water evaporation is favored. Fig. 2 shows the corresponding voltage and temperatures evolutions.

In this figure, some low-amplitude oscillations are observed on fuel cell stack temperature (±1 °C), that are

Table 1 – Technical characteristics of the used fuel cell.

Characteristic	Value
Membrane thickness	25 μm
Platinum load (anode & cathode)	0.4 mg cm^{-2}
Gas diffusion layer thickness	420 μm
Porosity	84%
Flow channel (geometry) used	Serpentine
Compressive force/torque used to assemble the stack	8 Nm
Reactant stoichiometry ratio (anode/cathode)	Nominal = 2/4
Gas purities	Hydrogène with max 8 ppm impurety (<3 ppm H_2O, <1 ppm O_2, <0.5 CO + CO_2, <5 ppm N_2)
Ion resistivity of DIW used for humidification of reactants	Deionized eau with conductivity < 10 μS cm^{-1}

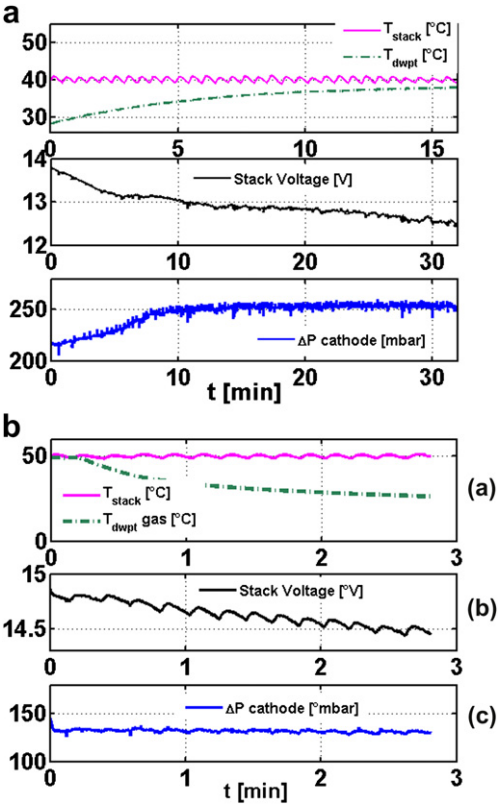

Fig. 2 – Evolution of temperatures, (a) voltages and pressure drop in case of deliberated flooding and (b) deliberated drying out experiments.

directly linked with the temperature regulation system used on the test bench.

Fig. 2 shows that stack voltage drop is a common consequence of both the flooding and drying out, while the cathode pressure drop only increases in case of flooding (Fig. 2a). Oppositely, cathode pressure drop remains unchanged in case of drying out (Fig. 2b). Therefore, the first parameter will act as fault detection basis and the second as discrimination parameter.

4. Neural network model presentation

4.1. *Recurrent Neural Networks*

A Neural Network (NN) consists of a number of processing units (neurons) that communicate by sending information to each other. The link between two neurons is done via weighted connections.

The most common neural network is the multilayer perception (MLP) [18]. For this type of NN, each unit performs a biased weighted sum of the inputs and sends it to a transfer function. The output is then an activation level reached by this function. The neurons are organized in a set of parallel layers and in feed-forward networks, all input signals flow in one direction, from input to output.

Once the topology (i.e. number of layers and number of neurons within these layers) is fixed, the network's weights are set by training algorithms that aim at minimizing the difference between the output calculated by the neural network and the experimental one. The most popular algorithm is back-propagation [19].

However, feed-forward networks can only perform static mapping between an input and an output space and can not take into account a temporal evolution. For that purpose, recurrent neural networks can be considered. In such networks, the outputs of some neurons are fed back, either to the same neurons or to neurons in the preceding layers. This implies that signals can flow both in forward and backward directions and that outputs at a given instant reflect the input at that instant as well as previous inputs and outputs. This makes the recurrent NNs particularly suitable for dynamic systems.

First introduced by Elman in 1990 [20], the Elman NN (ENN) is a recurrent neural network that has three layers: input, hidden and output layers (cf. Fig. 3). The feedback connections go from the outputs of neurons in the hidden layer to a special copy layer called "context" that constitutes a kind of "storage" of previous state of the hidden layer. This context layer allows the Elman neural network to detect and generate time-varying patterns, like the recurrent networks. However, Elman network presents the advantage of using back-propagation algorithm [18] for the training while this is not possible with other recurrent networks where the training algorithms are more complex and therefore slower.

The Elman network has sigmoid neurons in its hidden layer, and linear neurons in its output layer. The structure and mathematical description of Elman recurrent neural network are described in previous papers [16,21]. In this work, we used the neural network toolbox of Matlab® software [22].

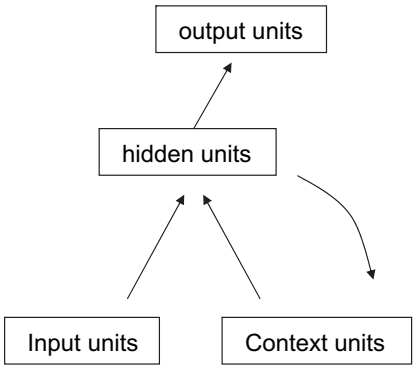

Fig. 3 – Scheme of the Elman neural network principle.

4.2. *Model presentation*

The aim of the Elman NN-based model presented in this work is to calculate the nonlinear relation between its inputs and outputs, in case of normal operation mode (without defaults).

The choice of input data is crucial for the Neural Network training results. The most influent variables in the water management must be included while the less influent data should be discarded, taking into account that a high number of inputs induces a complex and slow-to-run model. Based on the failure trees represented in Fig. 1, we choose the following variables to predict the NN output: applied current I, that can be measured by an LEM sensor, air inlet flow rate Q, that can be determined from the compressor speed, stack temperature T_{stack}, that can be measured by a thermocouple (placed for instance at the cooling circuit outlet) and dew point temperature T_{dwpt}. The last two parameters reflect the inlet relative humidity.

On the other hand since the model outputs are voltage $U(V)$ and pressure drop ΔP(mbar), the proposed model can easily be implemented on an on-board system adapted to transportation application.

We choose in this work to construct two individual Elman recurrent networks, the first one to predict the stack voltage and the second for the pressure drop, in order to adapt the complexity of each NN to the corresponding output. The hidden layers of first and second networks respectively contain 20 and 30 neurons. Note that no accurate method permits to choose the optimal number of neurons in the hidden layer. Our choice has been done on a "trial-error" going from a small number of neurons and increasing until a good compromise between model's complexity and performances is reached.

4.3. *Data collection*

The data set is split randomly into three independent sub-sets with the following proportion: 70% training, 20% validation and 10% test. The subdivision is done in such a way that each subset contains the same proportion of data from each operating condition as in the initial data set. The ENN was first trained with the first data set (training). Validation data permit avoiding the over-learning that leads to bad generalization capacities and the test set, which has never been seen by the

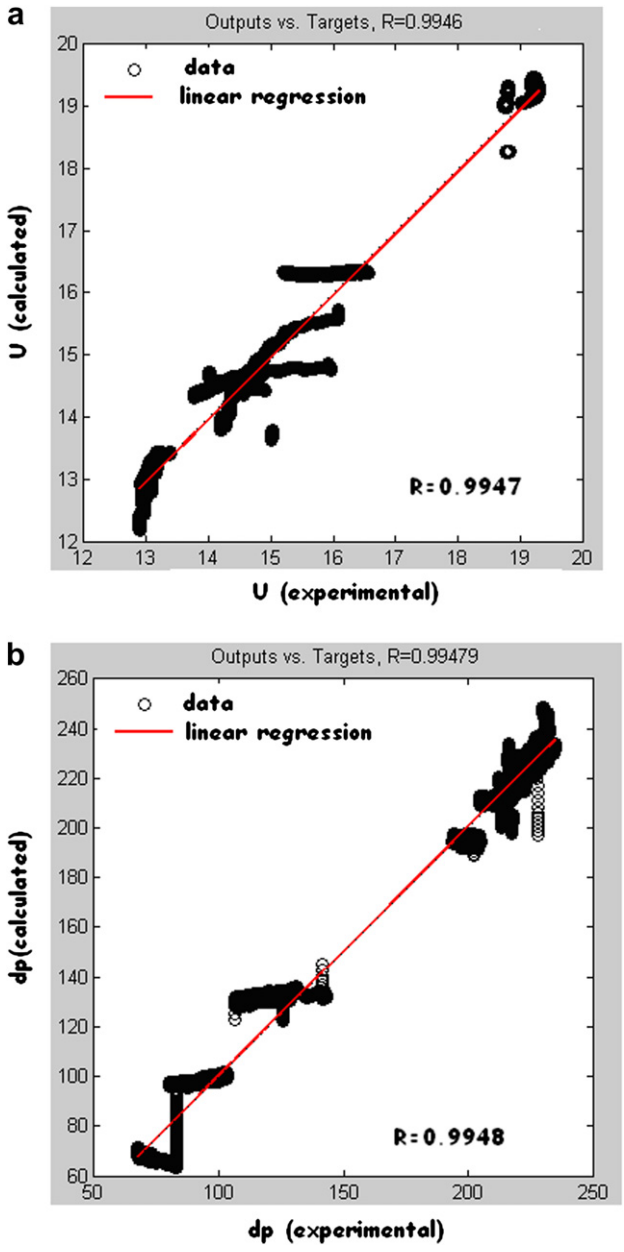

Fig. 4 – Linear regression between the network response and the corresponding experimental value for: (a) Voltage and (b) Pressure drop.

NN, permits evaluating the performance in generalization of the NN.

A data pre-processing is performed in order to normalize them between 0 and 1 (coded values) so as to facilitate the network training: normalization of the inputs ensures homogenized ranges and allows comparing the various weights related with different factors. Therefore, neglecting critical data with small absolute value is avoided. The NN outputs are renormalized to return in the correct range.

4.4. *Performance of the NN*

The mean squared error of the difference between the responses values calculated by the NN ($\hat{Y}$) and the experimental ones (Y) were calculated using the Matlab® software. The performance of the ENN was evaluated by performing a linear regression between both experimental and calculated values and assessed by the corresponding *Pearson correlation coefficient* R. This fitting's results are subject to statistical analysis in order to explain the relationship between the two data sets. The closer is R to 1, the better the correlation between $\hat{Y}$ and Y is: $R = 0$ means that the correlation is unpredictable. Mathematical details about the linear regression can be found in a previous work [16]. The linear regression for voltage and pressure drop, together with the corresponding Pearson coefficient, is respectively presented in Fig. 4a and b.

Fig. 4 shows the relationship between the experimental values and the results of the model, for different operating conditions (different clusters). The Pearson correlation coefficients are respectively 0.9947 and 0.9948 for stack voltage and pressure drop. The corresponding mean squared errors are respectively 0.0016 and 0.0022.

Fig. 5a and b gives the evolution of the calculated and experimental stack voltage and pressure drop for data belonging to the test set.

5. Diagnosis procedure based on the neural network model

Figs. 6 and 7 describe the proposed diagnosis methodology. As mentioned above, the neural network previously described was trained with data obtained in normal operating conditions: it has therefore been trained to recognize a normal

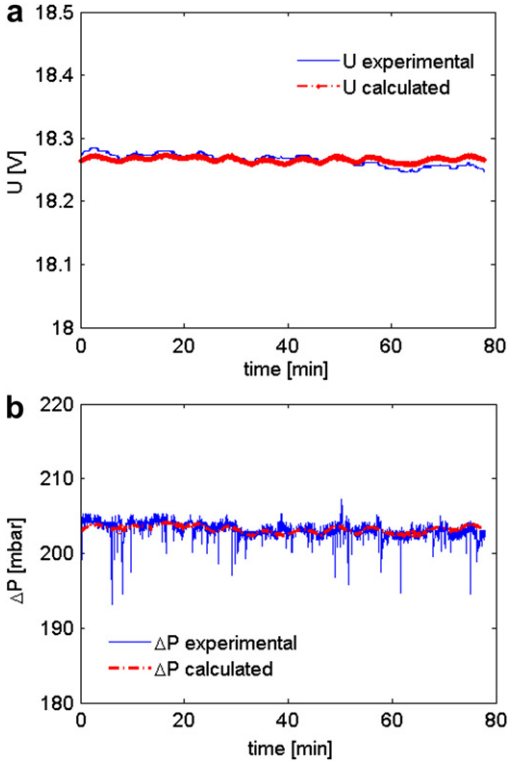

Fig. 5 – Evolution of the calculated and (a) experimental stack voltage and (b) pressure drop for data belonging to the test set (I = 0A, Qair = 52 NL.min^{-1}, Tsat = 35°C, Tstack = 40°C).

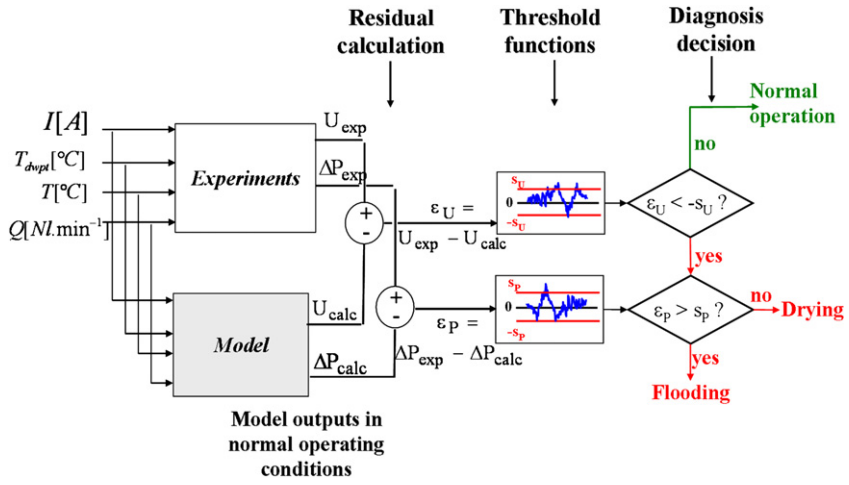

Fig. 6 – Description of the general diagnosis procedure.

operation. As a consequence, each deviation of experimental variables from predicted value can be interpreted as an abnormal operation mode. For that purpose, residuals ε_U and $\varepsilon_{\Delta P}$ are respectively calculated for voltage and pressure drop, according to the following equations:

$$\varepsilon_U = U - U_{exp} \text{ and } \varepsilon_{\Delta P} = \Delta P_{exp} - \Delta \hat{P} \quad (1)$$

where $\hat{U}$ and $\Delta\hat{P}$ respectively correspond to the values predicted by the model in normal operating conditions.

In addition, so as to take a relevant decision concerning a potential deviation of any variable's experimental value from model predicted ones, threshold values have to be defined on the basis of these residuals in their "normal" range of variation. We define threshold value as the value up to which, the residual is considered still in the normal operation range (its deviation is due only to measurements and model errors and not to an actual fault). These threshold values are then defined according to the following rule:

$$s_U = \max\left(\overline{\varepsilon_U} + 3\sigma(\varepsilon_U)\right) \text{ et } s_{\Delta P} = \max\left(\overline{\varepsilon_{\Delta P}} + 3\sigma(\varepsilon_{\Delta P})\right) \quad (2)$$

where $\overline{\varepsilon_x}$ et $\sigma(\varepsilon_x)$ are respectively the mean and the standard deviation of the residual related to x, (where x is U or ΔP). Eq. (2) uses normal operation data. It is supposed that the noise due to the measurements and the model errors is included in the "$3\sigma(\varepsilon_x)$". Since we used all the training set of data, taking the maximal threshold permits to consider the worst case over all the samples. With respect to the training set, these two values are: $s_{\Delta P} = 0.14$ mbar et $s_U = 0.12$ V.

In Eq. (2), the "$3\sigma(\varepsilon_x)$" value has been chosen empirically after trial-error rule. However, assuming that residuals' evolutions in case of normal operation are only due to measurements and/or regulation noise, their time distributions can be considered as normal. As a consequence, when one of them goes out the range of $\pm 3\sigma$, the probability of wrong fault detection is limited to 0.6%. Moreover, since a parameter's sense of evolution is significant in only one direction (decrease in case of voltage and increase in case of pressure drop), the probability of wrong fault detection is further reduced to 0.3%. Such a probability can be considered as low enough for an algorithm reliability regarding to fault detection.

As shown in both Figs. 6 and 7, our algorithm tries to detect the occurrence of a voltage residual value ε_U, below the threshold value s_U. If the residual remains above the threshold, it allocates the "Normal Operation". Otherwise, it indicates the presence of degradation. Then it examines the residual $\varepsilon_{\Delta P}$ related to pressure drop and compares its values to the corresponding threshold $s_{\Delta P}$. If the algorithm calculates a residual higher than the threshold, it identifies a flooding. Otherwise, it identifies a drying out.

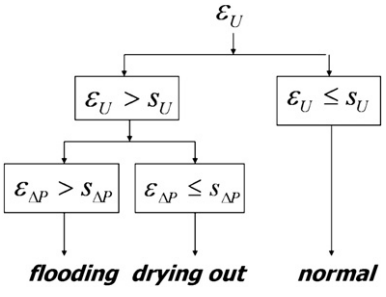

Fig. 7 – Classification rule according to the residuals analysis.

6. Results: diagnosis test

Fig. 8 shows the succession of deliberately flooded and drying out states. Fig. 8a shows the evolution of stack and gas dew point temperature. The flooding states are simulated by decreasing gas dew point temperature, while the drying out states are obtained by increasing its dew point temperature. The transition between two faulty states is a mitigation, leading to a temporary normal operation mode. Note that the stack temperature is maintained constant (50 °C) during the whole experiment.

Fig. 8b and c respectively shows the experimental and calculated by the NN values of stack voltage and pressure drop. The generated residual as well as the corresponding threshold are represented in Fig. 8d and e.

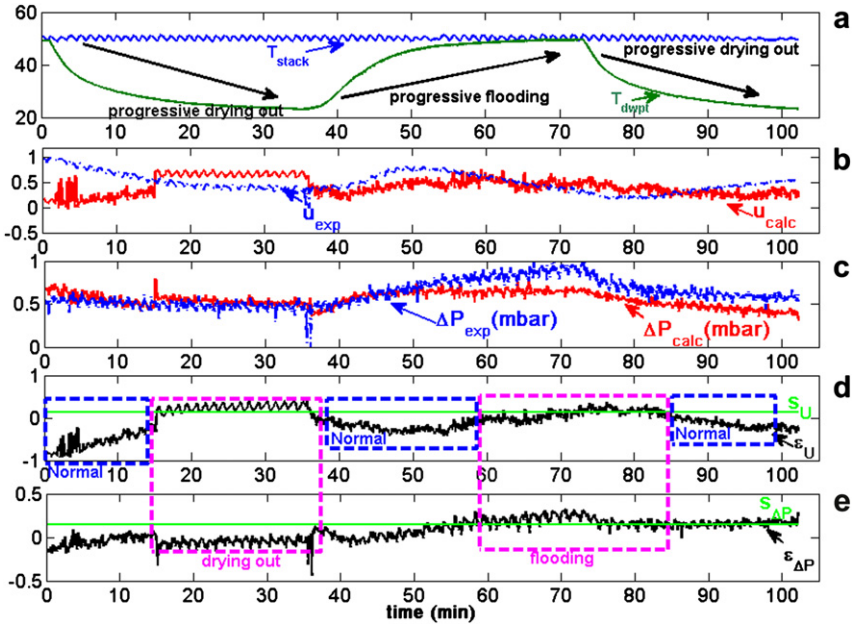

Fig. 8 – Simulation of three successive states of drying out, flooding and drying out: (a) evolution of the stack and air dew point temperature; (b) calculated and experimental voltages; (c) calculated and experimental cathode pressure drops; (d) residual on voltage and threshold; (e) residual on pressure drop and threshold.

At the beginning of the simulation, the gas dew point temperature is decreased below the stack temperature. This favors water evaporation and therefore induces a drying out state (between 0 and 35 min). The model detects a drying state between 15 and 35 min.

Then, gas dew point temperature is increased back close to stack operating temperature (between 35 and 75 min) in order to favor water condensation. It first permits the membrane rehydration and its recovery from drying out state (between 35 and 55 min), but, beyond a given time of operation during which stack and gas dew point temperatures are close, a flooding occurs. This flooding is diagnosed by the model between about 60 min and 86 min, because experimental and calculated pressure drop diverged.

After 75 min, dew point temperature is decreased back, favoring again water evaporation and therefore mitigating the flooding. The model detects a normal operation 10 min after. This can be explained by the time required to eject and evaporate the excess of accumulated water. Here, the cell recovers from flooding and the voltage begins to increase, which leads to a lower residual on voltage (below the fixed threshold) indicating a healthy operation mode.

7. Conclusion

In this paper, a diagnosis procedure related to drying out and flooding issues in PEFC stacks has been proposed. The presented model-based diagnosis procedure is based on the comparison between measured and calculated voltages and pressure drops by an Elman Neural Network, trained with data recorded in normal operation conditions.

The used procedure is based on some operation parameters as input parameters (namely current, stack and gas inlet temperatures, air flow rate) and some non-intrusive and easy-to-monitor parameters as output (namely, voltage and pressure drop between inlet and outlet of cathode compartment).

The physical parameters used in this model can be easily estimated even in an autonomous or embedded fuel cell system, which allows the proposed diagnosis method to be easily adapted to an on-board system, avoiding difficult and costly instrumentation inside fuel cell stacks or systems.

Acknowledgments

The authors would like to thank the French National Research Agency (ANR), in the scope of its National Action Plan for Hydrogen (PAN-H) for financially supporting this work.

REFERENCES

[1] Wilkinson DP, St-Pierre J. Durability. In: Vielstich W, Lamm A, Gasteiger H, editors. Handbook of fuel cells: fundamentals technology and applications. England: Wiley; 2003. p. 611–26.

[2] Yousfi Steiner N, Moçotéguy P, Candusso D, Hissel D, Hernandez A, Aslanides A. A review on PEM voltage degradation associated with water management: impacts, influent factors and characterization. J Power Sources 2008; 183:260–74.

[3] St Pierre J, Wilkinson DP, Knights S, Bos ML. Relationships between water management, contamination and lifetime degradation in PEFC. J New Mater Electrochemical Syst 2000; 3:99–106.

[4] BiyIkoglu A. Review of proton exchange membrane fuel cell models. Int J Hydrogen Energy 2005;30:1181–212.
[5] Merida W, Harrington DA, Le Canut JM, McLean G. Characterization of proton exchange membrane fuel cell (PEMFC) failures via electrochemical impedance spectroscopy. J Power Sources 2006;161:264–74.
[6] Roy SK, Orazem ME. Analysis of flooding as a stochastic process in polymer electrolyte membrane (PEM) fuel cells by impedance techniques. J Power Sources 2008;184: 212–9.
[7] Jemei S, Hissel D, Pera MC, Kauffmann JM. On-board fuel cell power supply modeling on the basis of neural network methodology. J Power Sources 2003;124: 479–86.
[8] Kumbur EC, Sharp KV, Mench MM. A design tool for predicting the capillary transport characteristics of fuel cell diffusion media using an artificial neural network. J Power Sources 2008;176:191–9.
[9] Lobato J, Cañizares P, Rodrigo MA, Linares JJ, Piuleac C-G, Curteanu S. The neural networks based modeling of a polybenzimidazole-based polymer electrolyte membrane fuel cell: effect of temperature. J Power Sources 2009;192: 190–4.
[10] Larminie J, Dicks A. Fuel cell systems explained. 2nd ed. Chichester: John Wiley & Sons; 2003.
[11] Taniguchi A, Akita T, Yasuda K, Miyazaki Y. Analysis of degradation in PEMFC caused by cell reversal during air starvation. Int J Hydrogen Energy 2008;33:2323–9.
[12] Yousfi Steiner N, Moçotéguy P, Candusso D, Hissel D. A review on PEM fuel cell catalyst degradation and starvation issues: causes, consequences and diagnostic for mitigation. J Power Sources 2009;194:130–45.
[13] Gerbec M, Jovan V, Petrovcic J. Operational and safety analyses of a commercial PEMFC system. Int J Hydrogen Energy 2008;33:4147–60.
[14] He W, Lin G, Nguyen TV. Diagnostic tool to detect electrode flooding in proton-exchange-membrane fuel cells. AIChE J 2003;49:3221–8.
[15] Barbir F, Gorgun H, Wang X. Relationship between pressure drop and cell resistance as a diagnostic tool for PEM fuel cells. J Power Sources 2005;141:96–101.
[16] Yousfi Steiner N, Candusso D, Hissel D, Mocoteguy P. Model-based diagnosis for PEFCs. Math. Compt Simult 2010;81: 158–70.
[17] Hissel D, Péra M-C, Candusso D, Harel F, Bégot S. Characterization of polymer electrolyte fuel cell for embedded generators. Test bench design and methodology. In: Zhang X-W, editor. Advances in fuel cells. Research Signpost, North Carolina State Univ.; 2005. p. 127–48.
[18] Bishop CM. Neural networks for pattern recognition. Oxford: Clarendon Press; 1995.
[19] Haykin S. Neural networks: a comprehensive foundation. Upper Saddle River (New Jersey): Prentice-Hall; 1999.
[20] Elman JL. Finding structure in time. Cogn Sci 1990;14: 179–211.
[21] Seker S, Ayaz E, Türkcan E. Elman's recurrent neural network applications to condition monitoring in nuclear power plant and rotating machinery. Eng Appl Artif Intelligence 2003;16: 647–56.
[22] Mathworks, www.mathworks.com, [accessed 01.01.10.].